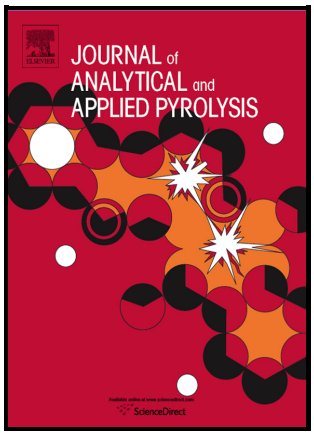

Thermochemical Recycling of End-of-life and Virgin HDPE: A Pilot-Scale Study

Mehrdad Seifali Abbas-Abadi, Azd Zayoud, Marvin Kusenberg, Martijn Roosen, Florence Vermeire, Parviz Yazdani, Jonathan Van Waeyenberg, Andreas Eschenbacher, Francisco Jose Arraez Hernandez, Maja Kuzmanović, Hang Dao Thi, Uros Kresovic, Bert Sels, Peter Van Puyvelde, Steven De Meester, Mark Saeys, Kevin M. Van Geem

PII: S0165-2370(22)00184-X

DOI: https://doi.org/10.1016/j.jaap.2022.105614

Reference: JAAP105614

To appear in: *Journal of Analytical and Applied Pyrolysis*

Received date: 28 May 2022
Revised date: 7 July 2022
Accepted date: 12 July 2022

Please cite this article as: Mehrdad Seifali Abbas-Abadi, Azd Zayoud, Marvin Kusenberg, Martijn Roosen, Florence Vermeire, Parviz Yazdani, Jonathan Van Waeyenberg, Andreas Eschenbacher, Francisco Jose Arraez Hernandez, Maja Kuzmanović, Hang Dao Thi, Uros Kresovic, Bert Sels, Peter Van Puyvelde, Steven De Meester, Mark Saeys and Kevin M. Van Geem, Thermochemical Recycling of End-of-life and Virgin HDPE: A Pilot-Scale Study, *Journal of Analytical and Applied Pyrolysis,* (2022) doi:https://doi.org/10.1016/j.jaap.2022.105614

Thermochemical Recycling of End-of-life and Virgin HDPE: A Pilot-Scale Study

Mehrdad Seifali Abbas-Abadi[1], Azd Zayoud[1], Marvin Kusenberg[1], Martijn Roosen[2], Florence Vermeire[1], Parviz Yazdani[1], Jonathan Van Waeyenberg[3], Andreas Eschenbacher[1], Francisco Jose Arraez Hernandez[1], Maja Kuzmanović[1], Hang Dao Thi[1], Uros Kresovic[4], Bert Sels[3], Peter Van Puyvelde[5], Steven De Meester[2], Mark Saeys[1], Kevin M. Van Geem[1,*]

[1] Laboratory for Chemical Technology (LCT), Department of Materials, Textiles and Chemical Engineering, Faculty of Engineering & Architecture, Ghent University, B-9052 Zwijnaarde, Belgium;

[2] Laboratory for Circular Process Engineering (LCPE), Department of Green Chemistry and Technology, Faculty of Bioscience Engineering, Ghent University, B-8500 Kortrijk, Belgium;

[3] Center for Sustainable Catalysis and Engineering (CSCE), Department of Microbial and Molecular Systems (M²S), Faculty of Bioscience Engineering, KU Leuven, Celestijnenlaan 200F, 3001 Heverlee, Belgium.

[4] Indaver NV, Dijle 17 a, 2800, Mechelen, Belgium

[5] Soft Matter, Rheology and Technology (SMaRT), Department of Chemical Engineering (CIT), Faculty of Engineering Science, KU Leuven, Celestijnenlaan 200J, 3001 Heverlee, Belgium.

Abstract

Industrial-scale application of end-of-life plastic pyrolysis still faces significant problems, such as a lack of detailed knowledge on degradation mechanisms, parameters affecting the degradation, and formation pathways of the primary pyrolysis products. Today, the degradation mechanisms based on radical chain scission are insufficiently understood to explain the pyrolysis chemistry from feedstock-to-product comprehensively. In this study, the impact of operating conditions on the degradation

mechanism is evaluated by pyrolyzing end-of-life and virgin high-density polyethylene (HDPE) in a continuous pilot-scale unit at temperature and pressure ranges of 450-504 ºC and 0.1-2 bara. The pyrolysis products were analyzed based on the detailed product composition obtained using comprehensive two-dimensional gas chromatography (GC×GC). A simplified kinetic mechanism was proposed to describe the main production pathways of the various components by considering the weakest points along the polymer chain. The results showed that the chain-end scission mechanism is the main mechanism in the HDPE pyrolysis process, even at low temperatures and pressures in the studied ranges. The pyrolysis of virgin HDPE under sub-atmospheric pressure, 0.1 bara, at 464 ºC reactor temperature, yields the highest concentration of linear hydrocarbons in the pyrolysis oil (93.2 wt.%). At higher pressure and temperature, the cyclic and branched hydrocarbons had a higher share of up to 17.4 wt.% compared to 6.8 wt.% at vacuum pressure and lower temperature. Interestingly, the pyrolysis of end-of-life HDPE at atmospheric pressure and 450 ºC led to more cyclic and branched hydrocarbons (sum: 22.1 wt.%), as opposed to that of virgin HDPE which is more prone to the production of linear hydrocarbons at the studied conditions. Regarding the additives and contaminants, a large amount of different metals and halogen atoms in the ppm range were detected in end-of-life HDPE, of which a small amount was still found in the pyrolysis oil.

Keywords:

Virgin and End-of-life HDPE; Pilot plant experimentation; Thermochemical recycling; Kinetic modelling; Two-dimensional GC×GC; Pyrolysis

Graphical abstract

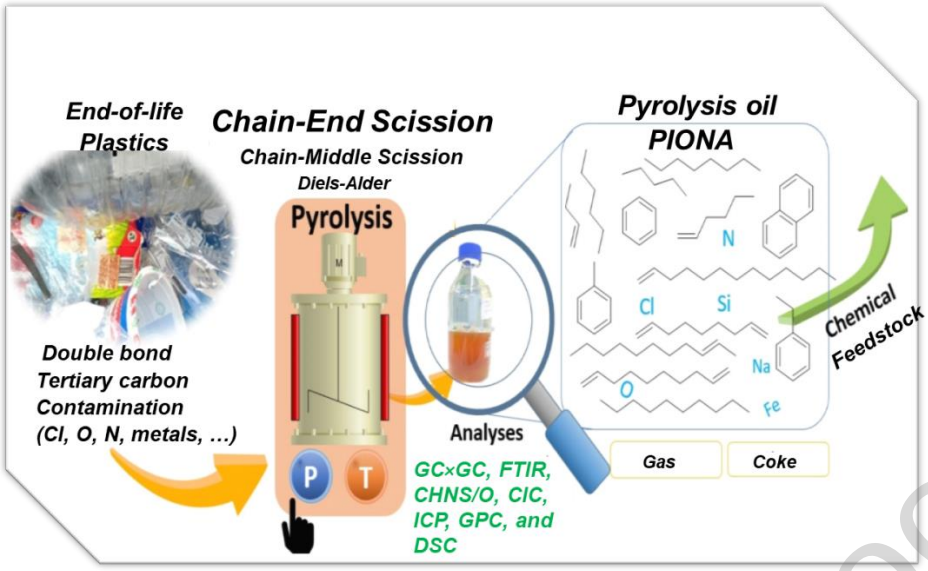

Abbreviations

amu	atomic mass unit
bara	absolute pressure
C_{av}	molar average carbon number
CIC	combustion ion chromatography
CSTR	continuous stirred tank reactor
DSC	differential scanning calorimetry
FID	flame ionization detector
g	gram
GC	gas chromatography
GC×GC	two-dimensional gas chromatography
GPC	gel permeation chromatography
H/C	hydrogen/carbon
HDPE	high density polyethylene
ICP-OES	inductively coupled plasma – optical emission spectrometry
LDPE	low density polyethylene
LLDPE	linear low density polyethylene
LOD	limit of detection

LOQ	limit of quantification
m	meter
MFI	melt flow index
min	minute
Mw	weight average molecular weight
Mn	number average molecular weight
MWD	molecular weight distribution
MS	mass spectrometry
n_{av}	weight average carbon number
P	Pressure
PDI	polydispersity index (Mw/Mn)
PE	polyethylene
PP	polypropylene
PS	polystyrene
PBR	polybutadiene rubber
PTV	Programmable Temperature vaporizing
qMS	quadrupole mass spectrometry
s	second
SI	supporting information
SSL	split/splitless
t	ton
T	temperature
TCD	thermal conductivity detector
UV	ultraviolet

1. Introduction

Polyolefins account for more than half of the world's plastics production (~356 $Mt \cdot y^{-1}$) and are commonly used in the disposable packaging industry [1]. The high sensitivity of polyolefins towards reprocessing leads to a significant loss of properties throughout mechanical recycling [2,3]. In addition, undesirable contaminants and additives, non-biodegradability, and the high cost of complete plastic sorting are reported to complicate mechanical recycling [4-6]. In general, the high degree of mixing and the resulting limitations of mechanical recycling mostly lead to lower quality recyclates i.e., downcycling [7]. Furthermore, strict food-contact regulations prevent the use of mechanically recycled products from their original application [8,9]. In this context, chemical recycling via pyrolysis may be a promising process to produce valuable products under different conditions [10-13]. Products of end-of-life plastic pyrolysis can be integrated into the petrochemical production scheme of virgin plastics closing the material loop [14-16]. In this way, production of light olefins from end-of-life plastics or using pyrolysis oil as feedstock for steam cracking plants leads to a far lower carbon footprint than other possible disposal methods, such as landfill or incineration [17-20].

High-density polyethylene (HDPE) is one of the commodity polymers, which is produced in various extrusion and/or injection grades. These grades are different in terms of molecular weight (Mw), molecular weight distribution (MWD), and comonomers (e.g., 1-butene, 1-hexene, and/or 1-octene) [21-23]. The type, amount, and distribution of comonomers play a key role in determining important physical and mechanical properties of HDPE such as density [24,25]. Thermal degradation studies of polyolefins show that the higher concentration of tertiary carbons as present in lower density polyethylene results in lower thermal stability, more chain scission, and decomposition products with shorter chains [21,26].

Besides the impact of the plastic structure on the pyrolysis products, the operating parameters play a vital role in the pyrolysis process. For instance, moderate temperatures during HDPE pyrolysis (less than 500 ºC) lead significantly to high molecular weight hydrocarbon products in the wax range (C_{21+}) [27-29]. Further increasing the pyrolysis temperature intensifies the mono- and bi-molecular reactions [27,30,31] and decreases the final product molecular weight [32-34]. Bimolecular reactions such as Diels-Alder result in the formation of naphthenes, aromatics, and polyaromatics (coke) [35-37]. Green and Sadrameli [38] investigated the impact of temperature from 400 to 1000 °C on the HDPE degradation in a fluidized bed reactor. The increasing temperature resulted in lower molecular weight products, while the concentration of cyclic products and coke formation increased clearly. In particular, the production of symmetric and/or stable hydrocarbons such as ethylene, methane, aromatics, and coke increased with increasing temperature. In contrast, the other hydrocarbons, such as C_{3+} olefins and C_{2+} paraffins, and naphthenes showed a maximum presence in the studied temperature range.

The pressure impact on HDPE pyrolysis has been studied less than the temperature effect. While most pyrolysis processes are usually reported at atmospheric pressure, it has been indicated that the pyrolysis pressure is another crucial factor of the polyolefin pyrolysis process. Studies carried out by Murata et al., [39] Cheng et al., [40] and Kumari and Kumar [41] confirm that the increased operating pressure leads to a higher concentration of reactants in the reactor, resulting in intensified molecular collisions and bimolecular reactions [39-41]. Murata et al. [39] investigated the effect of pressure between 1 and 8 bara on the thermal pyrolysis of polyethylene using a continuous stirred tank reactor (CSTR). Their results showed that pressure has a significant effect on the degradation mechanisms and pyrolysis products. The elevated pressure during pyrolysis can be a potential alternative for catalytic pyrolysis to narrow the product distribution and convert end-of-life plastics into lighter liquid

hydrocarbons. Cheng et al. [40] studied the effect of pressure between 1 and 51 bara on the pyrolysis of LDPE in a stirred reactor. Increased pressure intensified chain scission and secondary reactions, resulting in lighter products with more aromatics, naphthenes, and branched hydrocarbons and lower olefin concentrations.

The residence time in the reactor is one of the critical parameters in plastic pyrolysis. With increasing residence time, the product is re-exposed to primary and secondary reactions, which leads to a decrease in molecular weight and an increase in the formation of naphthenes, aromatics, and coke. For the reactor design, the residence time is one of the critical parameters, and should ideally be minimized while maintaining complete conversion [42,43].

Different environmental degradation reactions, such as mechanical stress, UV light, water, heat, aging, *etc.*, result in branching, double bonds and oxygenated chains in the structure of end-of-life plastics. The increasing presence of double bonds and oxygenated components over time leads to plastics yellowing and sometimes blackening if severe degradation would occur [44,45]. Various metals in end-of-life plastics, which are in minor amounts because of different additives and contaminants, can significantly affect the pyrolysis process. In the catalytic pyrolysis or subsequent catalytic upgrading of pyrolyzates, the metal contaminants can irreversibly deactivate the catalyst active sites. Therefore, it may be required to decontaminate the plastics or pyrolyzates before direct contact with catalysts [19,20,46-48].

The detailed characterization of end-of-life plastics pyrolysis products can, on the one hand, help to assure the feedstock quality for industrial processes and, on the other hand, help researchers in investigating the process chemistry and the effectiveness of various process parameters. Comprehensive two-dimensional gas chromatography (GC×GC) coupled with a flame ionization detector (FID) is one of the most accurate techniques to obtain the detailed compositions of hydrocarbon mixtures. In turn, the results obtained from GC×GC can assist

in predicting the impact of various process parameters on the final products, based on which processes can be scaled up to an industrial scale. Determining precise reaction mechanisms can accelerate the transition of various pyrolysis processes to industrial scale and steer the operating conditions to maximize the yield of desired products [49-51].

Given the importance of polyethylene pyrolysis, a complete study containing a comprehensive consideration of HDPE (end-of-life and virgin) and their respective pyrolysis products along with influential process parameters such as temperature and pressure was performed using a pilot-scale experimental setup. Hence, a comprehensive analysis was performed using GC×GC–qMS, GC×GC-FID, fourier-transform infrared spectroscopy (FTIR), CHNS/O elements analyser, combustion ion chromatography (CIC), inductively coupled plasma – optical emission spectrometry (ICP-OES), gel permeation chromatography (GPC), and differential scanning calorimetry (DSC) of pyrolysis oils produced from virgin and end-of-life HDPE to gain a detailed understanding of the pyrolysis oil quality and the effect of varying process conditions. In the following, the effect of different degradation mechanisms such as chain-end scission on the degradation of HDPE is presented. Furthermore, the effect of tertiary carbons and double bonds in determining the position of chain scission as well as pyrolysis products are indicated. In addition, we propose a kinetic model based on a quantum chemistry study, taking the effect of these parameters on the individual pyrolysis products into account. The work paves the way towards industrializing the HDPE pyrolysis process with a stronger and deeper understanding of the degradation pathways.

2. Materials and Methods

2.1. Materials and standards

The virgin HDPE 25055E as injection grade with a melt flow index (MFI) of 25 (g/10min @190 ^{o}C/2.16 kg, ASTM D1238) and density of 955 kg·m^{-3} was supplied by the DOW chemical company.

The post-consumer HDPE was a pelletized end-of-life HDPE film provided by ECO-oh! (Belgium). All HDPEs were applied in the pellet form.

Carbon disulfide (≥ 99 %, Sigma-Aldrich, Belgium) was used to dilute the waxy samples before GC×GC analyses. For the quantitative analysis purpose, 3-chlorothiophene (Sigma-Aldrich, Belgium) was used as an internal standard, with a minimum purity of 96 %. Helium, nitrogen, hydrogen, carbon dioxide, air, and oxygen were used as analytical gases with a minimum purity of 99.999 % (Air Liquide, Belgium).

2.2. Apparatus and experimental procedure

The pyrolysis experiments were performed using a pilot-scale pyrolysis unit under continuous feeding mode developed in-house at the Laboratory for Chemical Technology (LCT, Ghent University, Ghent 9052, Belgium). Step-by-step progress in the pyrolysis process and taking bigger steps is one of the research priorities in the pyrolysis field. Hence, in this paper, instead of using laboratory setups, the challenges and problems of the pyrolysis process were investigated on a pilot-scale plant. As shown in Figure 1, the pilot-scale unit consists of three main sections, namely, feeding, reaction, and condensation units. The feeding section consists mainly of the single screw extruder (LabTech, Thailand) with a panel for controlling the temperature (PID controllers) of extruder segments (150-190-230-280 °C) and screw speed (55 rpm for end-of-life HDPE and 65 rpm for virgin HDPE) to achieve the desired flow rate (2 $kg \cdot hr^{-1}$) for virgin and end-of-life HDPE. In this section, the feedstock was melted and injected into a 5.7 L volume, wall-heated CSTR Parr reactor (Model: 4584, U.S.A) via a heated connecting tube. The operating pressure in the reactor and condensation section was controlled using either nitrogen gas and a back pressure regulator (pressure more than 1 bara) or vacuum pump (pressure less than 1 bara) depending on the desired operating pressure. Furthermore, in order to evacuate the reactor from air, it was flushed with nitrogen before each experiment. The unit was designed to operate over a wide range of 0.1 to 20 bara. The reactor operating temperature was controlled using SpecView software and a PID controller. The range of selected temperature (450-504 °C) and pressure (0.1-2 bara) was such that the impacts of process and structural parameters on the final products could be investigated with a minimal number of experiments. In most studies [11,12],

temperatures between 450-500 ℃ have led to the maximum pyrolysis oil (as the research target) with a suitable residence time. Furthermore, high pressures have resulted in producing more pyrolysis gas and coke [39,40]. Consequently, regarding the high accuracy and sensitivity of the pilot-unit used with a minimum temperature gradient, a limited effective range was considered for temperature and pressure. In the following, to compare the structural differences between virgin and end-of-life polyethylene, the pyrolysis of end-of-life polyethylene was performed at an optimum point of 450 ℃ and atmospheric pressure. In the next step, to obtain the optimal points in the pyrolysis process, the contour plot by Minitab software was used.

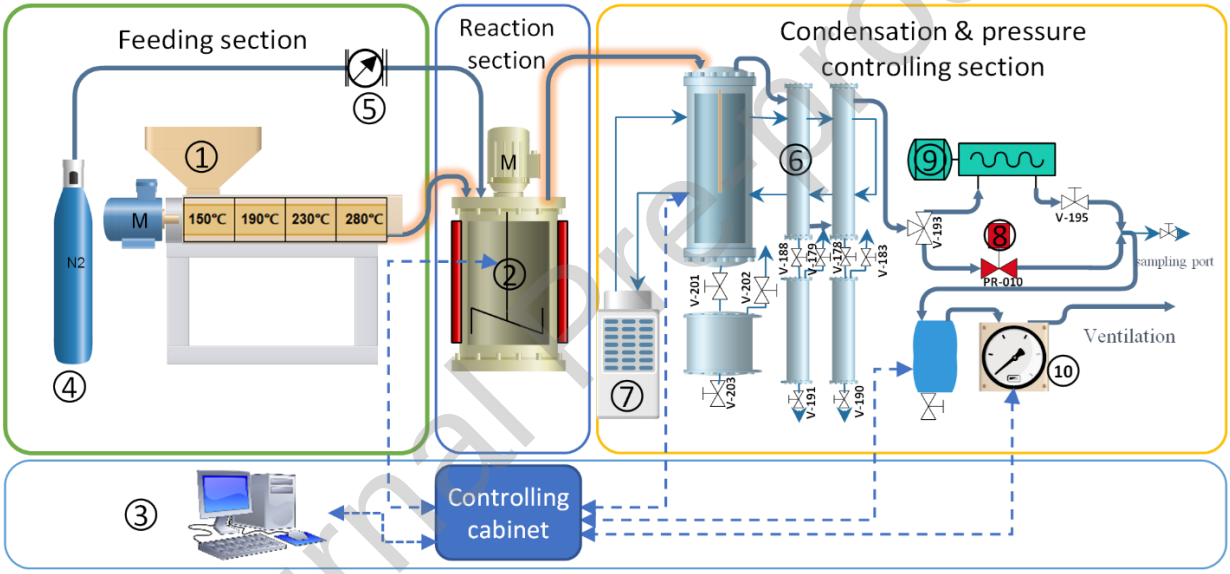

Figure 1. Pyrolysis pilot plant: (1) extruder, (2) continuous stirred tank reactor, (3) controlling unit, (4) inert gas (N_2) cylinder, (5) N_2 volumetric flow controller, (6) condensers, (7) cooler, (8) back pressure controller, (9) vacuum pump, (10) off-gas flowmeter (Adapted from [52]).

To provide uniform heat and mass transfer, a fixed stirrer speed of 500 rpm was used in the reactor. The evaporated products from the reactor were collected as condensed liquid products in the condensation section, while the non-condensable products were vented. In the studied temperature and pressure ranges, the thermal pyrolysis products of HDPE were in the form of a semi-solid wax; consequently, the first condenser temperature was set to 85 ℃ during the experiments to avoid blockage of the downstream tubes and to discharge the liquid products. Meanwhile, the remaining condensers were set at 20 ℃ to capture the lighter products. A volumetric gas flow meter (RITTER, Germany) was used to measure the flow of non-condensable products. The remaining solid residue in

the reactor was weighted separately after the completion of each experiment. The ratio of the remaining char to the feed consumption determined the share of char formation (wt.%). In general, in the long pyrolysis experiment of contaminated plastics, the high char formation can even prevent the stirrer from moving due to char sticking to the side walls near the stirrer blade. Certainly, for the industrial process, it must be possible to remove the formed char continuously during operation.

Analytical method

Gel permeation chromatography (GPC)

Analyses were performed on an Agilent 1260 Infinity II High-Temperature GPC automated system equipped with a 40-position carousel autosampler, high-sensitivity refractive index detector, viscometer detector, and light scattering detector. Three PLgel Olexis 300×7.5 mm columns were used in series. The temperature of the oven was set at 160 ℃, and 1,2,4-Trichlorobenzene (TCB) containing 5.7×10^{-1} mM of butylated hydroxytoluene (BHT) was used as eluent with a flow rate of 1.0 $mL\cdot min^{-1}$. Spectra were collected for over one (1) hour and analyzed using the Agilent GPC/SEC Software by viscometry analysis, using narrow polystyrene standards (Agilent PS-H EasiVial 2 mL pre-weighed Polystyrene Calibration Kit) ranging between 162 and 6×10^{6} $g\cdot mol^{-1}$.

A 1260 Infinity II High-Temperature sample preparation system was used to prepare the samples with an approximate concentration of 2 $mg\cdot ml^{-1}$. The samples were dissolved in TCB at a temperature of 160 ºC with shaking for one hour (for end-of-life HDPE samples, dissolution was conducted for 4 hours). The samples were filtered on 2 μm stainless steel frits and transferred to the corresponding sampling vials using a hand pipettor heated to 160 ℃, supplied with the sample preparation device. After their preparation, the samples were transferred to the GPC autosampler, which kept them at the sampling temperature.

In this paper, weight average molecular weight (Mw), number average molecular weight (Mn), and polydispersity index (Mw/Mn) as a function of MWD have been reported.

Fourier-transform Infrared spectrometry (FTIR)

Pellets of virgin and end-of-life HDPE were prepared prior to FTIR measurements. The HDPE samples with particle size of less than 150 µm were mixed with KBr with a ratio of 5 mg to 600 mg. The mixture was then pressed under three tons of pressure for two min to form a pellet. The FTIR spectrum of each pellet was obtained on a Bruker Tensor 27 FTIR spectrometer using a transmission cell from 600 to 4000 cm^{-1} with 64 scans at a resolution of 4 cm^{-1}.

Halogen analysis

Halogen analysis of the solid plastic samples was performed using combustion ion chromatography (CIC) according to the EN 14582 method. According to the ASTM standard D6470–99, halogen analyses of the waxy pyrolysis products were performed. The halogen (i.e. chlorine, bromine and fluorine) concentrations in the final solution were determined with ion chromatography (930 Compact IC Flex, Metrohm, Herisau, Switzerland), equipped with a Metrosep A Supp 7-250/4.0 column and conductivity detector. Quantification was performed based on linear calibration curves using 5 standard solutions in the range of 0 and 50 ppmw of the analytes of interest.

Metal analysis

Metal analysis was performed via inductively coupled plasma – optical emission spectrometry (ICP-OES) on a Thermo Scientific iCAP 7200 model, equipped with Qtegra Software (Thermo Scientific iCAP 7000 Plus Series ICP-OES, Thermo Fisher Scientific Brand, USA) and a CETAC AXP 560 autosampler (Teledyne Technology, USA). Standards for calibration (ranging from 0.001 ppmw up to 20 ppmw) were prepared using Certipur multi-element standard solutions (100 mg l^{-1} in 10 % HNO_3), containing Co, Cd, Cu, Li, Zn, Mg, Mn, Pb, Sr, Sb, Ti, Tl, Se, Ca, Ni, Mo, V, Be, As, K, Al, Fe, Hg, Si, Na, and Cr. Before ICP-OES analyses, an Anton Paar (Graz, Austria) Multiwave 5000 microwave oven equipped with a 20 SVT-rotor and PTFE-TFM digestion vessels was used to digestive the samples (0.50 ± 0.05

g). Subsequently, 3.0 mL of double-distilled water and 10.0 ml of concentrated HNO_3 (70 %, Sigma Aldrich) were added to the weighed sample. The vessels in the microwave oven were subjected to the following heating program: 20 min ramping time up to a temperature of 200 ºC and 15 min heating time. After digestion, the samples were diluted to a volume of 50 mL with double-distilled water. The blank tests were performed using the same procedure without the addition of a sample. Afterwards, the samples were filtered using a syringe filter (0.45 μm syringe filter, PP filter media, CHROMAFIL). The limit of detection (LOD) of the ICP-OES analysis was quantified by multiplying the standard deviation of the blank by 3. The limit of quantification (LOQ) was quantified by multiplying the standard deviation of the blank by 10. The values for the LOD and LOQ are given in the SI.

Comprehensive two-dimensional gas chromatography (GC×GC)

The detailed composition of six HDPE pyrolysis products was characterized using comprehensive two-dimensional GC×GC. The Thermo Scientific TRACE GC×GC setup (Interscience, Belgium) was composed of an Mxt-1 column (60 m × 0.25 mm × 0.25 μm) as the first column connected to a ZB-35HT (2.2 m × 0.18 mm × 0.18 μm) as the second column through ferrule kits (SilTite™, Thermofisher, Belgium). The column set and a dual-state cryogenic liquid CO_2 modulator were placed in the same oven. The outlet of the second column was connected to an FID or a qMS detector. In GC×GC, as shown in Figure 2, the components are first separated in the first column based on the boiling point, and in the second column, the components are separated based on polarity.

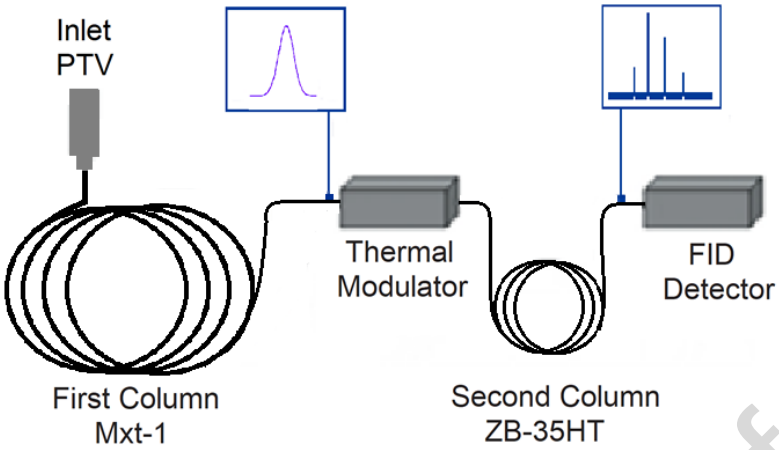

Figure 2. Schematic of a GC×GC system.

The identification of components in the six HDPE samples was performed by using the GC×GC - qMS setup. While the GC×GC - FID was used for quantitative analysis based on the internal standard calibration method and effective carbon number approach explained in detail elsewhere [49,50,53]. In this paper, 3-chlorothiophene was used as internal standard. For the GC×GC - qMS setup, the data acquisition rate was set at 30 spectra s^{-1} with the scanning range set from 30 to 400 amu. The GC×GC -qMS transfer line temperature was set at 280 ºC, and the ion source temperature was set at 300 ºC. The MS detector used electron ionization (70 eV). For the GC×GC - FID setup, H_2, air, and N_2 (make-up gas) flow rates were set at 35, 350, and 35 ml·min^{-1}, respectively. The FID temperature was set at 350 ºC, and the data acquisition rate was 100 Hz. Helium was used as a carrier gas at a constant flow rate. A summary of GC×GC parameters applied in this work is given in where yieldi is the weight fraction of compound i; wt.%$_{IS}$ is the weight fraction of internal standard; fi is the relative response factor of compound i, which is calculated based on effective carbon number approach; fIS is the relative response factor of the internal standard (3-chlorothiophene), which is determined as 1.94 based on the calibration; ai is the peak area of compound i; and aIS is peak area of the internal standard.

Table 1. Peak integration of the different components was performed using GC image software and the yield of components was calculated by [54]:

$$Yield_i(\%) = \frac{f_i \times a_i}{f_{IS} \times a_{IS}} \times wt.\%_{IS} \quad (1)$$

where $yield_i$ is the weight fraction of compound i; $wt.\%_{IS}$ is the weight fraction of internal standard; f_i is the relative response factor of compound i, which is calculated based on effective carbon number approach; f_{IS} is the relative response factor of the internal standard (3-chlorothiophene), which is determined as 1.94 based on the calibration; a_i is the peak area of compound i; and a_{IS} is peak area of the internal standard.

Table 1. Overview of GC×GC - FID/MS settings (Mxt-1 × ZB-35HT).

	GC×GC - FID	GC×GC - qMS
Injector	PTV*	SSL
Temperature (ºC)	370	300
Split flow (ml·min^{-1})	10	10
Carrier gas (ml.·min^{-1})	2.1	2.1
Oven start (ºC)	40	40
Oven end (ºC)	400	400
Ramp (ºC)	2	2
Modulation time (s)	6	6
Detector temperature* (ºC)	350	300
Detector range (-)	1	-
Detector acquisition rate (Hz)	100	30

*Temperature corresponds to the final temperature of the temperature program

Elemental (CHNS/O) analysis

CHNS/O analysis of solid plastic feedstocks and the waxy products was performed using a Flash EA2000 elemental analyzer (Interscience, Belgium) equipped with a TCD. According to the ASTM D 5291 standard method in combustion mode, CHNS analysis was performed to determine carbon, hydrogen, nitrogen, and sulfur. According to the ASTM D 5622 standard method, oxygen determination was performed in a separate reactor in pyrolysis mode. The CHNS/O composition of the samples was derived based on at least three repeat analyses of each sample.

Differential Scanning Calorimetry (DSC) measurements

DSC measurements were obtained on a DSC Q2000 (TA Instruments) apparatus. 8-10 mg samples were heated and cooled between -80 and 150 ºC in aluminum hermetic pans. After each cycle, the samples were kept isothermal for 5 minutes, and a heating rate of 10 ºC·min^{-1} was kept between -50 and 150 ºC. Each sample completed the heating and cooling cycle two times since the first cycle eliminates any thermal history of the sample.

Results and Discussion

Virgin and End-of-life HDPE composition

HDPE film grades, which were used in the present study as end-of-life HDPE, usually have a lower density (higher comonomer content) than the present injection grade virgin HDPE. Additionally, since the end-of-life HDPE consists of a few percent of other polyolefin constituents [55], a higher amount of tertiary carbons was present in the post-consumer HDPE sample compared to the virgin HDPE sample. Besides the presence of tertiary carbon atoms, oxygenated components, double bonds, and crosslinked chains (depending on the extent of plastic aging) in end-of-life HDPE could also affect the final product composition [44,45].

The elemental composition of the plastic samples processed in this study are shown in Table 2. In virgin and end-of-life HDPE, the calculated H/C ratio was as expected to be similar, 0.1668 and 0.1604 respectively. The lower H/C ratio of the end-of-life HDPE can be an indication of higher

amounts of unsaturation compared to virgin HDPE. Regarding the saturation structure of polyolefins (C_nH_{2n+2}, n_{av}>3500), the maximum H/C ratio amounts to (2n+2/12n) ~0.167. For end-of-life plastic samples consisting predominantly of polyolefins (i.e. >97 %), the H/C ratio does not differ much from 0.167. Due to additives (antioxidants), contamination with residues or missorted plastics such as PET and/or oxidative degradation, the oxygen content of the end-of-life HDPE sample amounts to 0.2 wt.%, whereas for the virgin sample, it was below the detection limit. The measured elemental compositions show that the end-of-life HDPE is rich in heteroatoms and metals. These elements can be related to the initial structure of HDPE (catalyst, additives), incomplete plastics sorting, additives and fillers, and different contaminants related to the plastic's lifetime.

Ziegler-Natta (generally: $TiCl_4/MgCl_2/AlEt_3$) [56] and Philips (Cr_2O_3/SiO_x) [57] catalysts are used to produce commercial HDPE, and traces of the catalyst remain in the polymer product. Heat stabilizers (generally: calcium stearate and zinc stearate) [58] and antioxidants [59] are commonly added as additives to HDPE during extrusion. Consequently, some elements, such as Ti, Mg, O, Cl, Al, Cr, Si, Zn, Ca, P were detected in virgin HDPE (Table 2).

Table 2. Elemental compositions of the end-of-life and virgin HDPE. CHNS/O was measured using organic elemental analysis; halogens were measured using CIC; metals were measured using ICP-OES. LOD and LOQ values of the different methods can be found in SI.

	Virgin HDPE	End-of-life HDPE
Element	Concentration [wt.%]	
N	<LOD	<LOD
C	85.7	86.0
H	14.3	13.8
S	<LOD	<LOD
O	<LOQ	0.2
Element	Concentration [ppmw]	
Cl	n.d.	920
F	n.d.	500

Br	n.d.	<50
Al	<LOQ	169.3
As	4.5	<LOQ
Be	<LOD	<LOD
Ca	109.1	1409.3
Cd	0.2	0.7
Co	<LOQ	0.7
Cr	5.2	4.6
Cu	4.8	7.5
Fe	35.0	105.3
Hg	<LOD	<LOD
K	<LOQ	131.2
Li	<LOD	0.2
Mg	6.5	160.4
Mn	0.5	1.9
Mo	<LOD	<LOQ
Na	<LOQ	155.2
Ni	3.1	2.9
Pb	<LOQ	7.3
Sb	<LOD	<LOD
Se	<LOD	<LOD
Si	11.1	218.1
Sr	<LOQ	1.9
Ti	6.7	73.8
V	<LOD	<LOD
Zn	9.5	50
Total metals	196.2	2500.3

The most prominent metals in the end-of-life HDPE were Ca, Si, Al, Mg, Na, K, Fe, and Ti. Aluminum foils (incomplete sorting) and other aluminum constituents can be sources of aluminum contamination [55]. Titanium oxide (as white pigment) [60] and carbon black (as black pigment) [61] are most commonly used as pigments in the plastics industry. Calcium carbonate and silica are often used as mineral fillers in many plastics products [62]. Sodium and chlorine in end-of-life plastic occur mainly due to the adsorption of salts from food residues and PVC labels. Other sources of metal elements are other polymers (PET, ABS, PA6,…), catalysts, additives, and metal-containing inks on paper and PVC labels [55].

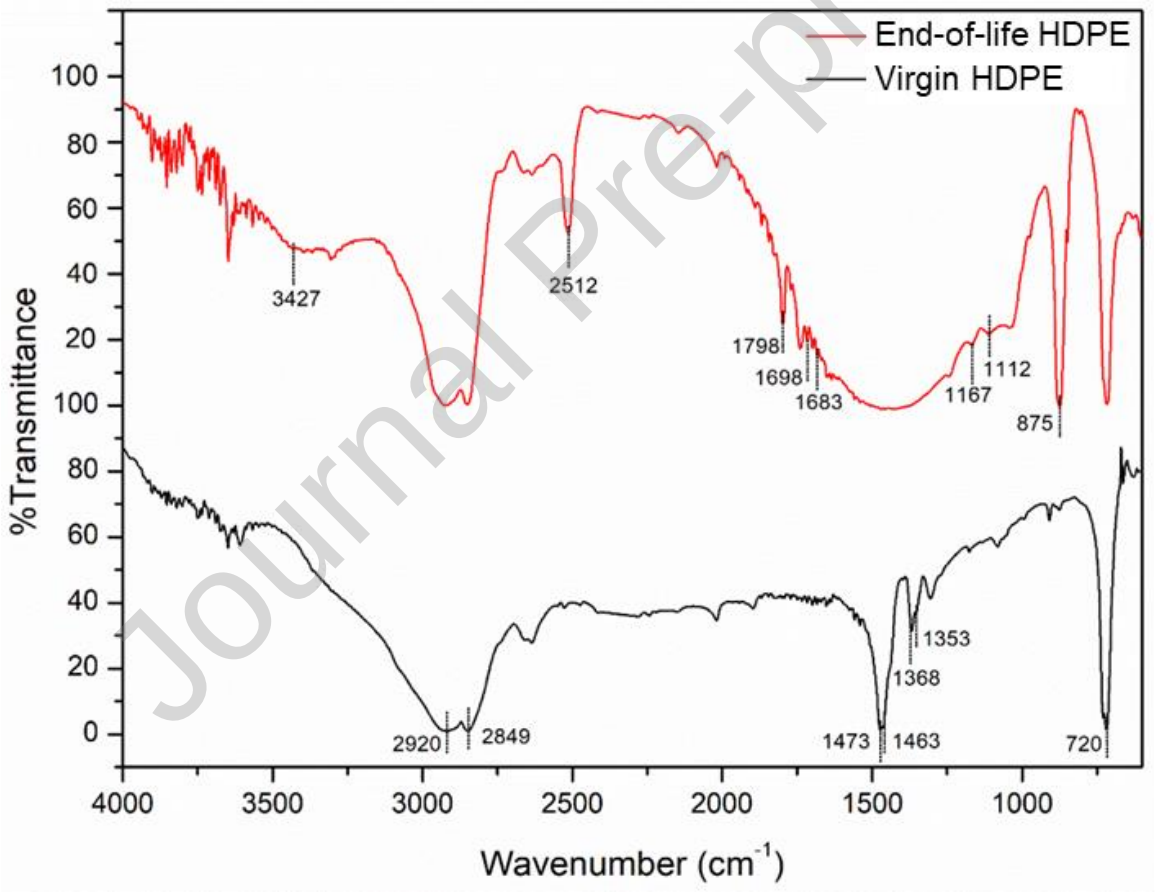

Figure 3. FTIR spectra of virgin (black line) and end-of-life (red line) HDPE.

The molecular structure of the virgin and end-of-life HDPE is studied using FTIR measurements and the resulting spectra are shown in the Figure 3. The characteristic methylene stretch and vibration peaks appear in the FTIR spectrum of both the end-of-life and

the virgin PE [63]. The peaks at 2920 cm^{-1} and 2849 cm^{-1} are assigned to the CH_2 asymmetric and symmetric stretches, respectively. The vibrational scissoring and bending of the methylene and methyl groups overlap in the FTIR spectrum of the virgin sample at 1440-1490 cm^{-1} showing two intense peaks at 1473 cm^{-1} and 1463 cm^{-1}. Rocking vibrations of the methylene groups appear near 720 cm^{-1}. The methylene rocking vibration peak is split into two peaks due to the close interaction of the packed methylene chains. The methyl group umbrella mode appears at 1368 cm^{-1} and confirms the presence of short hydrocarbon side chains terminated with methyl groups. The peak with lower intensity at 1353 cm^{-1} is assigned to the wagging deformation of the CH_2 groups [64].

The FTIR spectrum of the end-of-life HDPE sample contains the abovementioned characteristic peaks for polyethylene together with several new peaks which are assigned to the formation of C=C, C-O, and C=O. A broad peak appears in the spectrum of the end-of-life HDPE between 1000 to 2000 cm^{-1} due to the overlapping peaks of several chemical environments [63]. The vibration of the C=C groups appears at 875 and 3300 cm^{-1}. The formation of these groups is also confirmed by absorption bonds at 1683 cm^{-1} [63]. There is no clear peak or peak shoulder at 3037 cm^{-1} which might rule out the presence of aromatic hydrocarbons. Other vibrational modes of aromatics appear in the range of 1400-1700 cm^{-1} which is difficult to discuss due to peak broadening in this region. The C-O and C=O vibrational peaks appear near 1100 cm^{-1} and 1650 cm^{-1}, respectively, showing partial chain oxidation in the end-of-life sample [63]. Specifically, the peaks at 1167 cm^{-1} and 1698 cm^{-1} show the oxidation of the end-of-life sample, while these peaks are missing in the FTIR spectrum of the virgin HDPE. The low-intensity broad peak at 3427 cm^{-1} is associated with the presence of hydroxyl groups. The sharp peak at 2512 cm^{-1} might be due to the presence of calcite on the end-of-life sample [65]. To conclude, the FTIR spectrum indicates the presence

of double bonds and oxygenated moieties in the end-of-life HPDE as compared to the virgin sample.

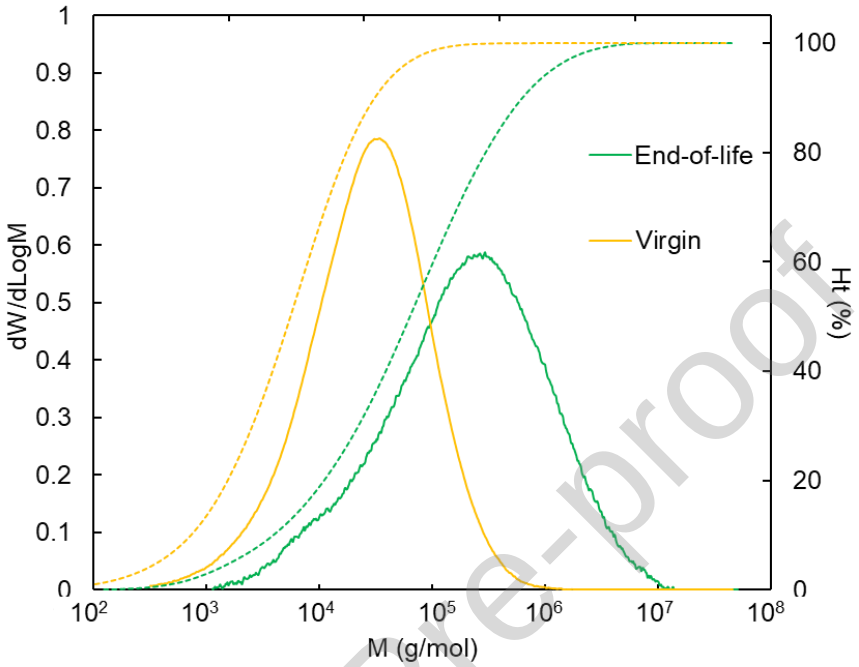

Figure 4. GPC graphs of the virgin and end-of-life HDPE.

Figure 4 shows GPC graphs of end-of-life and virgin HDPE (relative and cumulative distributions). Based on the GPC data, the end-of-life HDPE differed significantly from the virgin HDPE in terms of molecular weight (578623 vs. 51896 $g \cdot mol^{-1}$) and polydispersity index (11.76 vs. 4.62). In general, HDPE film grades (the end-of-life HDPE) have lower MFI (high Mw), and broader MWD than injection grades (the virgin) [66-68]. On the other hand, crosslink degradation during the extrusion and aging processes typically increase the molecular weight and broaden the MWD in end-of-life polyethylene [3,69].

The effect of temperature and pressure on the pyrolysis products

Figure 5 depicts the effect of the chosen process conditions on the product yields of gas (C_1-C_5), condensed product (C_5-C_{65}), and remaining char. Regarding the low boiling point and close to ambient temperature, C_5 was found in both pyrolysis oil and gas. The results indicated that with increasing pressure and temperature in the studied ranges, the production

of gas (4.9-12.3 wt.%) and char (0.3-0.8 wt.%) increased. Furthermore, with increasing pressure and temperature, the amount of condensed product has decreased substantially (95.1-86.9 wt.%). In accordance with the results, the literature study showed that pyrolysis oil has reduced with increasing temperature and pressure using different reactors e.g., CSTR and stirred pressurized autoclave reactor [39-41]. Due to the presence of oxygenated moieties and double bonds in end-of-life HDPE (see FTIR figure) and intensification of aromatization reactions, the formed coke (1.5 wt.%) was increased even at lower temperatures and pressures compared to virgin HDPE. Furthermore, more double bonds and tertiary carbons in the end-of-life HDPE resulted in intensifying the primary reactions and more gas (12.3 wt.%) production at atmospheric pressure and lower temperature compared to virgin HDPE in the studied range.

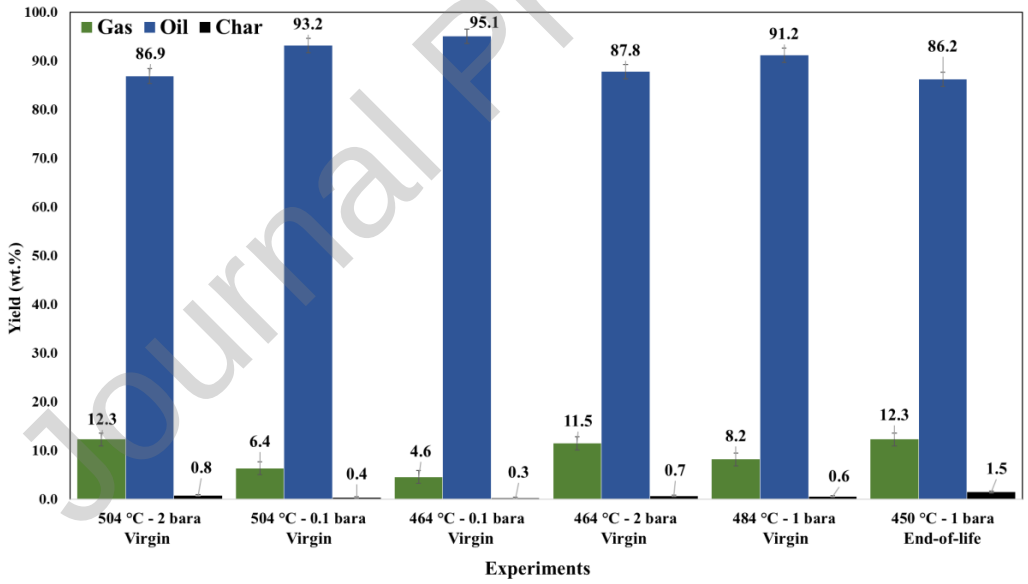

Figure 5. The effect of temperature and pressure on the products yield.

Figure S1 presents the contour plot of pyrolysis oil (a), pyrolytic gas (b), and pyrolytic coke (c) yields versus pressure and temperature. As shown in Figure S1(a), at sub-atmospheric pressures close to vacuum (<0.2 bara) and temperatures below 480 °C, the maximum pyrolysis oil could be produced (94 wt.%). In addition, increasing the pressure was more effective in reducing the pyrolysis oil than the temperature. At low pressures up to at least 92

wt.% of virgin HDPE could be converted to pyrolysis oil in the studied temperature range. In addition, the maximum produced gas occurred with more than 12% at the highest studied temperatures (> 500 ℃) and pressures (> 1.8 bara). In the case of gas production, the effect of pressure is far greater than temperature, and high pressures have a greater impact on gas production (Figure S1, b). Although the roots of coke formation and gas production are different, they behaved almost similarly and maximum coke formation occurred at high temperatures and pressures (>0.8 wt.%). The coke formation at low temperatures and pressures reached less than 0.3 wt.% (Figure S1, c). In general, increasing temperature and pressure led to intensifying the chain-end scission reactions (gas production), and the bimolecular reactions (coke formation).

As the first step in identifying pyrolysis oil, the DSC instrument was used to study the melting curves of the different pyrolysis oils (Figure S2). This is in contrast with pure wax materials, which lead to sharper peaks, as seen in ASTM D 4419 [70]. The broad melting profile can be explained by the large mixture of molecules with different molecular weights and structures. The influence of the pressure in the pyrolyzate virgin samples is visible, and lower pressures result in higher maximum melting temperatures (32-70 ℃) because of lower residence time and scission rate in polymer chains [39].

Figure 6 exemplifies the GC×GC-FID chromatogram of the condensed product of end-of-life HDPE pyrolysis. It shows that all chemical groups such as olefins (α-olefins, isoolefins), paraffins (n-paraffins, isoparaffins), diolefins, naphthenes, and aromatics (naphthenoaromatics, mono, and diaromatics) can be unambiguously distinguished from each other.

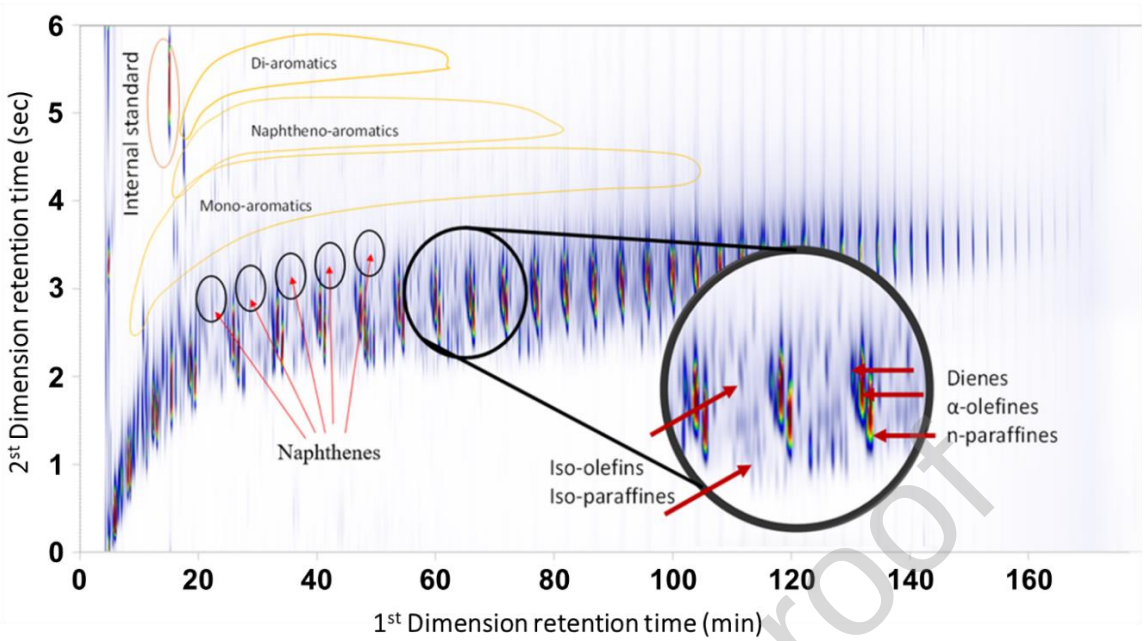

Figure 6. GC×GC-FID chromatogram of end-of-life HDPE pyrolysis oil (450 ºC, 1 bara).

Table 3 shows the different components of condensed products of virgin and end-of-life HDPE as a function of the process conditions. The results indicated that with increasing temperature and pressure, the liquid share of pyrolysis oil as a light fraction (C_{21-}) has increased (29.6-65.3 %), while the produced wax as a heavy fraction (C_{21+}) was decreased clearly (70.4-34.7 %). Furthermore, the light fraction accounted for 64.1 % of pyrolysis oil of end-of-life HDPE. Cheng et al. [40] have investigated the effect of temperature and pressure on light and heavy fractions of pyrolysis oil and produced gas using a stirred pressurized autoclave reactor. The results indicated that with increasing temperature and pressure, the produced wax was decreased and moved towards the production of lighter products.

Table 3. Hydrocarbon composition of the pyrolysis oils measured using GC×GC-FID.

HDPE type	Temperature (ºC)	Pressure (bara)	L.F (%)	H.F (%)	O (%)	P (%)	I.O (%)	I.P (%)	D (%)	N (%)	A (%)	L (%)	B (%)	C (%)	(O+I.O+D+C) /(P+I.P)
Virgin	504	2	65.3	34.7	38.2	30.9	4.2	1.8	13.5	10.3	1.1	82.6	6	11.4	2.1
Virgin	504	0.1	29.6	70.4	40.7	39.1	1	0.7	12.9	5.3	0.3	92.7	1.7	5.6	1.5
Virgin	464	0.1	33.6	66.4	39.5	39.7	1.1	0.8	13.6	5	0.3	92.8	1.9	5.3	1.5

Virgin	464	2	61.7	38.3	36	34.8	5.9	1.3	13.1	8.4	0.5	83.9	7.2	8.9	1.8
Virgin	484	1	48.1	51.9	38.7	34.6	3	1.5	13.5	8.1	0.6	86.8	4.5	8.7	1.8
End-of-life	450	1	64.1	35.9	33.7	33.3	6.7	2.3	10.9	11.8	1.3	77.9	9	13.1	1.8

L.F.: Light fraction (C_{21-}); H.F.: Heavy fraction (C_{21+}); O: Olefin; P: Paraffin; I.O: Isoolefin; I.P: Isoparaffin; D: Diolefin; N: Naphthene; A: Aromatic; L: Linear hydrocarbons (O+P+D); B: Branched hydrocarbons (I.O+I.P); C: Cyclic hydrocarbons (A+N)

In the HDPE pyrolysis, chain branching and dealkylation reactions are effective in producing isoolefins and isoparaffins. Increasing the pressure and reactant concentration in the reactor along with the residence time led to the intensification of bimolecular reactions such as chain branching [39]. However, bimolecular reactions were minimized due to faster leaving products under strong vacuum and better molecular dilution, which led to less branched products [30].

Given that some olefins and dienes participate in bimolecular reactions and become cyclic compounds [71], the ratio of unsaturated (olefin, isoolefin, diolefins) and secondary products (naphthene, and aromatic) to saturated compounds (paraffin and isoparaffin) should be considered. The results indicated that with increasing temperature and pressure, the mentioned ratio has increased from 1.5 to 2.1 (Table 3). This ratio is important because it reflects the overall rate of degradation reactions containing primary and secondary reactions.

Figure S3 shows the effect of temperature and pressure on the various components of pyrolysis oil using contour plots. As can be seen in the studied temperature range, the temperature had a limited effect on olefin (Figure S3, a), paraffin (Figure S3, b) and linear products (Figure S3, f) in general. What can be seen from the graphs is that at low pressures (< 0.3 bara) with minimum bimolecular reactions [30], more than 90% of the pyrolysis oil was linear hydrocarbons (Figure S3, f). On the other hand, Figure S3 (g) presented that in the studied ranges, the maximum of branched products (> 7%) appears at the highest pressures (≥ 1.8 bara) and low temperatures (< 470 ºC) while the minimum of branched hydrocarbons (≤

2%) were produced at vacuum pressures (0.1 bara). The concentration of branched compounds in the condensed product from end-of-life HDPE (9.0 %) was higher than in virgin HDPE (max: 7.2 %) in the studied ranges. Higher comonomer content in extrusion film grades (end-of-life HDPE), along with a few percent of other polyolefins in the end-of-life plastic, resulted in more branched components even at lower process pressure (1 bara) compared to virgin plastics at higher pressure (2 bara). Furthermore, mechanical and UV degradation in end-of-life polyethylene leads to chain branching and cross-linking reactions, increasing the production of branched compounds [45,72].

α,ω-diolefins are usually produced when an abstraction by a radical takes place from an olefin and then a β-scission happens of the formed radical, while conjugated dienes are formed by the scission in the β-position of double bonds. It cannot be avoided that a significant portion of conjugated dienes is converted to cyclic compounds via Diels-Alder reactions [40], it is thus rather difficult to discuss the effect of temperature and pressure on conjugated diene production (Figure S3, c). In the studied process conditions, the results showed that the produced diolefin concentrations of the virgin sample did not differ significantly. However, considering outstanding shares of cyclic compounds (5.6-13.1 %) and coke (0.3-1.5 wt.%) under different pyrolysis conditions, it appears that more dienes have been produced, some of which have been consumed as reaction intermediate.

Figure S3 (d, e) indicated at temperatures above 500 °C and pressures above 1.7 bara, the total of cyclic compounds reached over 11% while at vacuum pressures (< 0.6 bara) and low temperatures (< 475 °C) was minimized (~ 5%). Cyclic compounds in pyrolysis are produced by Diels-Alder and electrocyclic reactions. As the pressure and concentration in the reactor increase, the probability of recombination increases, and stable hexagonal rings are produced. Diels-Alder reactions require a cis-shaped conjugated diene that reacts with an olefin to form a cyclic compound [73]. Some of the cyclic compounds became aromatic by

dehydrogenation, which was increased by increasing temperature and pressure [74]. Additionally, due to Diels-Alder, electrocyclic reaction and other bimolecular reactions, some of the produced aromatics react further to produce polyaromatics ultimately leading to coke formation [75].

Figure 7 shows the distribution of different compounds of condensed products (C_{5+}), based on carbon number under different temperature and pressure ranges for virgin and end-of-life HDPE. Several observations can be made from these diagrams. The chains in the HDPE structure, which are free of comonomer, can form the longer pyrolysis products (C_{21+}), including linear α-olefins, n-paraffin, and α,ω-diolefins (Figure 7 a, b, c). In addition, the olefin/paraffin ratio has decreased in almost all cases with an increase in carbon numbers. It appears that under random chain scission, mostly the produced lighter chain tends to form olefins and the heavier chain tends to form paraffins. Furthermore, the share of heavy linear hydrocarbons has increased with decreasing temperature and pressure which is logical due to less severe cracking. In contrast, the percentage of light branched and cyclic hydrocarbons have increased with temperature and pressure.

It should also be borne in mind that some lighter olefins were converted to cyclic compounds under bimolecular reactions, and the ratio of olefin/paraffin in lighter hydrocarbons could be higher. In the pyrolysis oil, aromatics and naphthenes were found in low molecular weight and 1 to 3 rings (C_{30-}) (Figure 7 f, g). Due to the high boiling points of heavier aromatics, it is less likely that they leave the reactor, and consequently they turn into coke [76]. Hence, the pyrolysis of branched chains leads to higher isoolefin and isoparaffin production. The branched products were often found in the low molecular weight range due to the presence of side groups and their higher scission potential (Figure 7 d, e).

The study of the obtained products indicated that it is possible to produce a wide range of hydrocarbons in polyethylene pyrolysis by changing the process parameters, e.g., temperature, pressure, and residence time. As evaluated in other works, products with less cyclic compounds can be used both as pure and mixed (with light naphtha) feedstock for steam cracking units in the production of light olefins [77,78]. Furthermore, by increasing the temperature and pressure and producing more cyclic and nonlinear hydrocarbons, some commercial fuels can be produced by performing complementary processes i.e., hydrogenation [79].

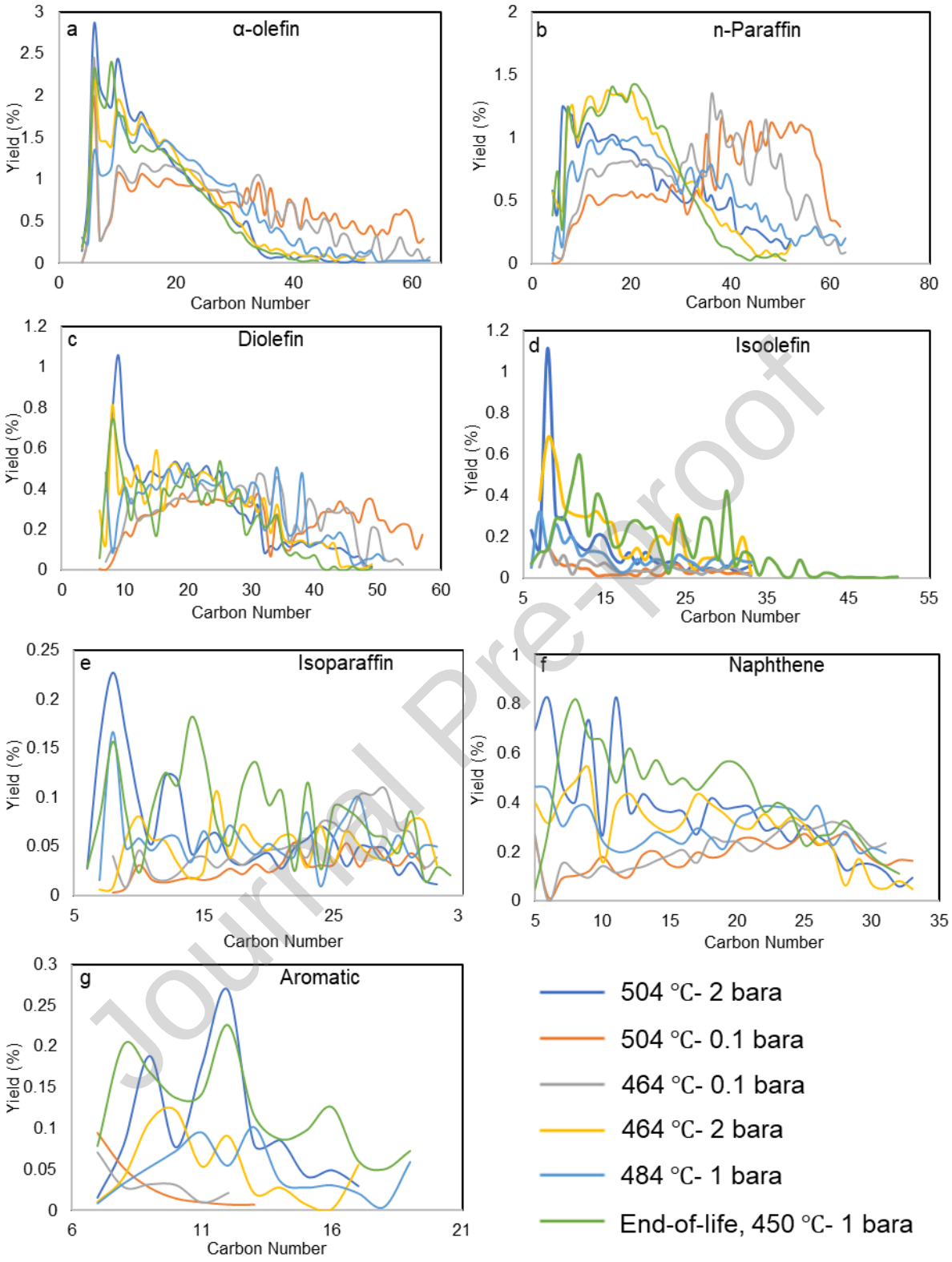

Figure 7. The yields of different pyrolysis products versus carbon numbers.

In an interesting study, Figure 8 presents the effect of temperature and pressure on the distribution of condensed products and the average carbon number (C_{av}). All graphs show that

the maximum carbon molar percentage of the pyrolysis products lies at 6 carbon atoms after which it decreases. What is noteworthy here is that ~ 28 to 39 carbon·mol.% (C·mol.%) of pyrolysis products that contain 1 to 5 carbon atoms are non-condensable. Therefore, it is indicated that chain-end scission is more likely to occur in HDPE pyrolysis than chain-middle scission even in the low temperature, and pressure ranges studied. Furthermore, the results indicate that with increasing pressure and temperature, the chain scission reactions were significantly increased, which led to a decrease in the carbon number of the final product (Figure 8, C_{av}: 22.4-13.1). The presence of double bonds and higher tertiary carbons in the end-of-life HDPE structure has led to lower thermal stability [77] and higher chain scissions than virgin HDPE. Consequently, at atmospheric pressure and lower temperature, the pyrolysis of end-of-life HDPE has led to a lighter product (C_{av}: 13.0).

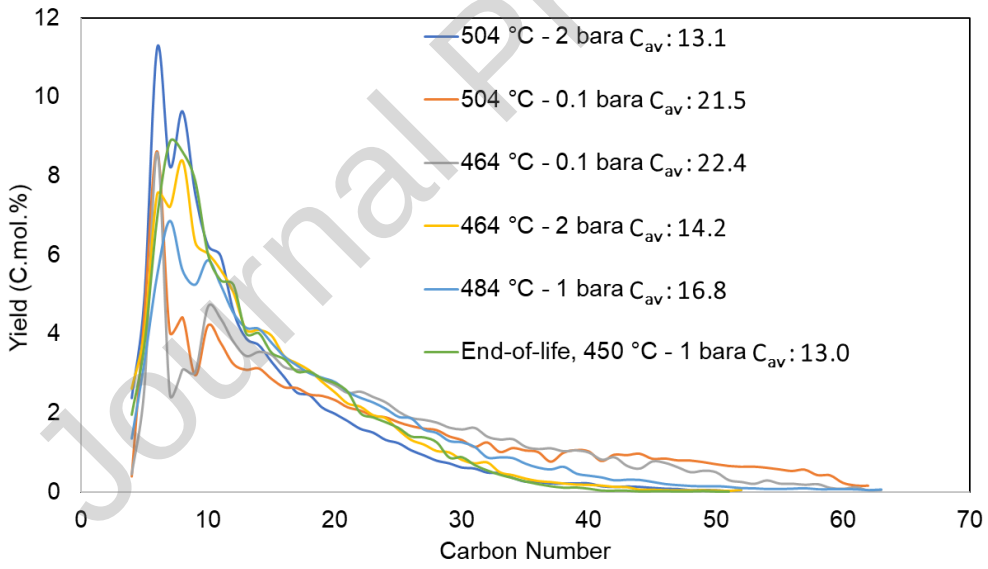

Figure 8. The carbon number distribution of the pyrolysis products under different temperatures and pressures.

Table 4. Hydrocarbon composition of the pyrolysis oils measured using GC×GC-FID.

HDPE type	Temperature	Pressure (bara)	C_1-C_6 (C·mol.%)	C_6-C_{12} (C·mol.%)	C_{13}-C_{21} (C·mol.%)	C_{21+} (C·mol.%)
Virgin	504	2	47	28	15	10

Virgin	504	0.1	40	17	15	28
Virgin	464	0.1	34	19	20	27
Virgin	464	2	47	24	17	12
Virgin	484	1	41	22	18	19
End-of-life	450	1	49	26	15	10

Table 4 shows the pyrolysis product composition based on the C·mol.%. As discussed, the chain-end scission mechanism plays a significant role in the HDPE pyrolysis. Since naphthenes, aromatics, and polyaromatics are mostly formed of light olefins [78,79], the percentage of chain-end scission can be higher than the measured values.

As can be seen in Table 4, with increasing pressure and temperature, the intensity of chain-end scission reactions (34-47 C·mol.%) increased and chain-middle scissions (28-10 mol.%), which lead to heavy products (C_{21+}), decreased significantly. The presence of double bonds and more comonomer in the end-of-life polyethylene structure resulted in more chain-end scission (49 mol.%).

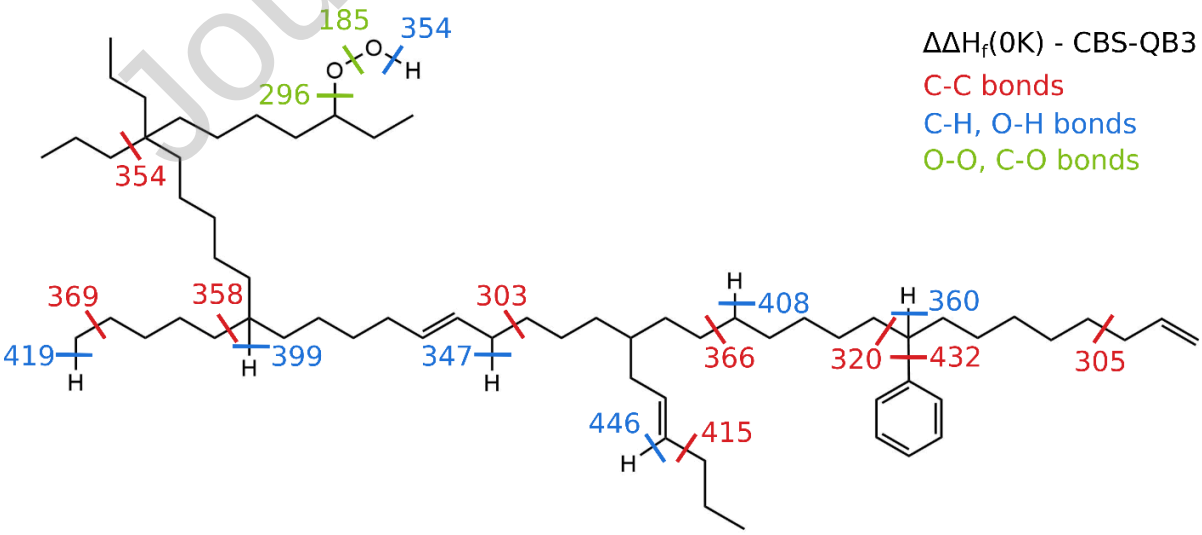

Figure 9. Bond dissociation energies (BDE) for common bonds in end-of-life polyolefin microstructures. Energies are calculated from the formation energies at 0K ($\Delta H_{f,0K}$) [kJ·mol^{-1}] for representative smaller molecules and radicals, calculated using quantum chemistry at the CBS-QB3 level of theory. For double bonds, the trans configuration is used.

Based on the experimental results, the composition of the starting HDPE and the presence of impurities affect the thermal decomposition of HDPE. Figure 9 presents the bond dissociation energies (BDE) for common bonds in polyolefin microstructures. Energies are calculated from the formation energies at 0 K ($\Delta H_{f,0K}$) [kJ·mol^{-1}] for representative smaller molecules and radicals in vacuum, calculated using quantum chemistry at the CBS-QB3 level of theory. Different C-C and C-H bond types that can be present in polyolefin microstructures are indicated in Figure 9 (red and blue, respectively). The difference in rotational rates leads to different dissociation energies between the C-C bonds discussed in Figure 9. Furthermore, a double bond rotation requires breaking the π bond and forming a carbene intermediate which occurs only at high energies close to the binding energy of a σ bond [80]. Lack of double bond rotation and placement in cis and trans structures can facilitate the scission in the β-position of the double bond.

Based on the experimental results and literature study, Figure S4 presents the proposed kinetic model that includes pathways for achieving all observed products. Deoxygenation, dealkylation, chain scission, and isomerization reactions are generally considered as common monomolecular degradation reactions (Figure S4, reactions 1-10) in polyolefins [44,45,72]. Due to a higher rotation rate in the backbone of hydrocarbon chains and lower dissociation energy compared to side groups, the breaking probability of side groups is much lower than the chain scission (Figure S4: reaction 3>> reaction 2) [81,82].

In terms of thermal stability, virgin and end-of-life polyethylenes differ in the amount of double bonds and oxygenated moieties as shown by the prior FTIR analysis. Furthermore, metal contaminants can play a catalytic role in end-of-life polyethylene degradation.

Regarding the low conductivity of polyolefins, the existing metal particles intensify the heat transfer by increasing the thermal conductivity. In addition, metal ions can reduce the activation energy of degradation by engaging with polyolefin chains[20,83,84].

The calculated dissociation energies (Figure 9: 303-415 $kJ \cdot mol^{-1}$) show that the probability of a bond scission in the β-position of a double bond is much higher than scission in α-position (Figure S4, reactions 4-5) [85]. α-bond scission can lead to the production of unstable vinyl radicals and alkynes upon a β-scission reaction (Figure S4, reaction 12), and scission in the β-position of the double bond leads to the production of resonantly stabilized radicals and furthermore to conjugated dienes (Figure S4, reaction 16). The C-H bond scission in the β-position of C=C with low dissociation energy (Figure 9: 347 $kJ \cdot mol^{-1}$) can help create a conjugated diene.

Reactions 17-21 comprehensively present cycling and aromatization (Figure S4). Diels-Alder reactions, including olefins and conjugated dienes, usually result in monocyclic naphthenes. However, the reaction of formed rings with conjugated dienes and other cyclic species (Figure S4, reaction 20) under certain conditions, leads to an increase in the number of rings. As the number of rings increases, the boiling point of the specie rises to the point where it is difficult to leave the reactor, while the number of its rings continues to increase and form the remaining coke (Figure S4, reaction 21) [86-88]. It should be noted that in end-of-life plastics, some mineral and organic contaminants are part of the char formed [20,48].

Differences in decomposition rate and products between virgin and end-of-life HDPE are thus affected by several factors such as the type of bond (single or double) [80], carbon type (secondary and tertiary) [26], freedom (chain-end or chain-middle) [39], stereoisomers (cis and trans) [85], steric hindrance [89], and temperature (rotation rate, molecular collision) [32]. The weakest point in hydrocarbons may occur in the vicinity of a double bond (Figure 9: β

position: 303-305 kJ·mol^{-1}) or a side group (Figure 9: 320, 354, 358 kJ·mol^{-1}). Without these influential factors, a chain scission with lower probability (Figure 9: 366 kJ·mol^{-1}) may occur based on the chain freedom (Figure S4: Reaction 6-8) [32,80,90]. Accordingly, carbon atoms at the chain-end have more freedom and rotation rate than carbon atoms in the middle of the chain. Consequently, as chain-end scission, light hydrocarbons usually make up a significant molar portion of the product. Light olefin production has a higher probability than the formation of light paraffins (Figure 9: 305 vs. 358-366 kJ·mol^{-1}) because of the rigid C=C bond at the end of olefins (Figure S4: Reactions 7-8) [39].

With decreasing the reactor pressure, thermodynamically, the boiling point of the produced hydrocarbons decreases and reaches a minimum at near-vacuum pressure [91]. For this reason, heavy produced hydrocarbons that can leave the reactor quickly under vacuum pressure, including minimal scission, may stay in the reactor longer and convert to lighter products with more aromatics and polyaromatic (coke) formation under high pressures [40,92,93].

Conclusion

Performing CHNS/O, DSC, CIC, ICP-OES, FTIR, GPC, GC×GC–qMS, GC×GC,-FID analysis provides detailed information on the end-of-life and virgin polyolefin characterization. The results obtained from the plastic feedstock characterization, along with the obtained pyrolysis products and the proposed thermal decomposition mechanism, showed that double bonds and tertiary carbons are the most important structural parameters affecting the thermal stability and pyrolysis product composition of HDPE and other polyolefins.

Taking into account typical operating conditions of potential industrial-scale processes, the temperature (450-504 ºC) and pressure (0.1-2 bara) ranges were evaluated, and the obtained products were investigated using comprehensive two-dimensional GC×GC-FID. The impact of pressure (0.1-2

bara) on the products was more significant than the processing temperature. The results indicated that in the studied ranges, pressure was more effective than temperature. Hence, if the goal of the pyrolysis process is to achieve heavy products with less cyclic products and coke formation, vacuum pyrolysis can be an option. However, to produce light products with high branched and cyclic concentrations, the pressure can be increased as much as possible. Furthermore, in the studied range, most of the scissions occurred at the chain-end, and with increasing temperature and pressure, the ratio of chain-end scission to the chain-middle scission increased clearly as demonstrated by the higher molar yields of low molecular weights.

Due to the higher content of double bonds (from aging) and comonomers in the structure of the end-of-life HDPE, pyrolysis resulted in lighter products and more branched and cyclic compounds than what was obtained with virgin plastic. The presence of catalytically active metals in the end-of-life HDPE sample may influence the thermal decomposition chemistry leading to higher amounts of polyaromatic hydrocarbons and ultimately coke in the reactor.

As a result, if advanced sorting could be implemented to selectively collect end-of-life HDPE with high density (>955 $Kg \cdot m^{-3}$), this would result in pyrolysis oils with a higher content of linear olefins and paraffins at low temperatures and pressures (vacuum). Higher pressures and temperatures lead to lighter hydrocarbons with more cyclic and branched hydrocarbons. In addition, end-of-life polyethylene is more suitable for producing branched and cyclic compounds (high octane fuels). In all cases a feedstock with a minimum content of olefins and cyclic compounds in the pyrolysis oil will lead to more light olefin production by steam cracking.

Finally, it may be concluded that the products of PE thermal pyrolysis are a suitable feedstock for upstream processes (e.g., steam cracking). However, in order to achieve a sustainable solution and solve the challenges, some complementary processes such as hydrogenation or mixing with fossil-based feedstocks such as naphtha must be considered. Furthermore, the production of other chemical products e.g., fatty alcohols, acids, and esters can be another useful solution for pyrolysis oils.

Author Contributions:

Authors	Conceptualization	Methodology	Software	Validation	Writing - Original Draft	Writing - Review & Editing	Supervision
Mehrdad Seifali Abbas-Abadi	*	*	*	*	*	*	
Azd Zayoud		*		*		*	
Marvin Kusenberg	*			*		*	
Martijn Roosen		*				*	
Florence Vermeire	*		*			*	
Parviz Yazdani		*				*	
Jonathan Van Waeyenberg		*				*	
Francisco Jose Arraez Hernandez		*				*	
Maja Kuzmanović		*				*	
Hang Dao Thi						*	
Uros Kresovic						*	
Andreas Eschenbacher						*	
Bert Sels						*	
Peter Van Puyvelde						*	
Steven De Meester						*	
Mark Saeys						*	
Kevin M. Van Geem	*	*		*		*	*

Acknowledgments

The research leading to these results has also received funding from the Fund for Scientific Research Flanders (FWO) and innovation program/ERC grant agreement no.818607 (OPTIMA). This work was also performed in the framework of the Catalisti cluster SBO project WATCH (HBC.2019.0001 "Plastic waste to chemicals") and P2PC (Plastics to Precious Chemicals) with the financial support of VLAIO (Flemish Agency for Innovation and Entrepreneurship).

Declaration of competing interest

The authors declare no conflict of interest.

References

[1] G. Faraca and T. Astrup, *Waste Management*, 95, (2019) 388.

[2] L.A. Pinheiro, M.A. Chinelatto and S.V. Canevarolo, *Polymer Degradation and Stability*, 86, (2004) 445.

[3] J. Dostál, V. Kašpárková, M. Zatloukal, J. Muras and L. Šimek, *European Polymer Journal*, 44, (2008) 2652.

[4] O. Horodytska, F.J. Valdés and A. Fullana, *Waste management*, 77, (2018) 413.

[5] K. Ragaert, L. Delva and K. Van Geem, *Waste management*, 69, (2017) 24.

[6] M. Okan, H.M. Aydin and M. Barsbay, *Journal of Chemical Technology & Biotechnology*, 94, (2019) 8.

[7] M. Hong and E.Y.-X. Chen, *Green Chemistry*, 19, (2017) 3692.

[8] V.S. Cecon, P.F. Da Silva, G.W. Curtzwiler and K.L. Vorst, *Resources, Conservation and Recycling*, 167, (2021) 105422.

[9] E. De Tandt, C. Demuytere, E. Van Asbroeck, H. Moerman, N. Mys, G. Vyncke, L. Delva, A. Vermeulen, P. Ragaert, S. De Meester and K. Ragaert, *Waste Management*, 119, (2021) 315.

[10] M.S. Abbas-Abadi, *Journal of Thermal Analysis and Calorimetry*, 143, (2021) 2867.

[11] M.S. Abbas-Abadi, M.N. Haghighi and H. Yeganeh, *Journal of Analytical and Applied Pyrolysis*, 95, (2012) 198.

[12] M.S. Abbas-Abadi, M.N. Haghighi and H. Yeganeh, *Fuel Processing Technology*, 109, (2013) 90.

[13] O. Dogu, M. Pelucchi, R. Van de Vijver, P.H. Van Steenberge, D.R. D'hooge, A. Cuoci, M. Mehl, A. Frassoldati, T. Faravelli and K.M. Van Geem, *Progress in Energy and Combustion Science*, 84, (2021) 100901.

[14] R. Xu, C. Yan, Q. Liu, E. Liu, H. Zhang, X. Zhang, X. Yuan, L. Han, H. Lei and R. Ruan, *Fuel Processing Technology*, 227, (2022) 107127.

[15] G.K. Parku, F.-X. Collard and J.F. Görgens, *Fuel Processing Technology*, 209, (2020) 106522.

[16] Y. Zhang, G. Ji, C. Chen, Y. Wang, W. Wang and A. Li, *Fuel Processing Technology*, 206, (2020) 106455.

[17] A. Eschenbacher, R.J. Varghese, E. Delikonstantis, O. Mynko, F. Goodarzi, K. Enemark-Rasmussen, J. Oenema, M.S. Abbas-Abadi, G.D. Stefanidis and K.M. Van Geem, *Applied Catalysis B: Environmental*, 309, (2022) 121251.

[18] A. Eschenbacher, F. Goodarzi, R.J. Varghese, K. Enemark-Rasmussen, S. Kegnæs, M.S. Abbas-Abadi and K.M. Van Geem, *ACS Sustainable Chemistry & Engineering*, 9, (2021) 14618.

[19] A. Eschenbacher, R.J. Varghese, M.S. Abbas-Abadi and K.M. Van Geem, *Chemical Engineering Journal*, 428, (2022) 132087.

[20] M. Kusenberg, A. Zayoud, M. Roosen, H.D. Thi, M.S. Abbas-Abadi, A. Eschenbacher, U. Kresovic, S. De Meester and K.M. Van Geem, *Fuel Processing Technology*, 227, (2022) 107090.

[21] M.S. Abbas-Abadi, M.N. Haghighi and H. Yeganeh, *Journal of applied polymer science*, 126, (2012) 1739.

[22] S. Ronca, in *Brydson's plastics materials*, Elsevier, 2017, p. 247.

[23] C. Vasile and M. Pascu, *Practical guide to polyethylene*, iSmithers Rapra Publishing, 2005, p.

[24] D.R. Burfield and N. Kashiwa, *Die Makromolekulare Chemie: Macromolecular Chemistry and Physics*, 186, (1985) 2657.

[25] L. Kurelec, M. Teeuwen, H. Schoffeleers and R. Deblieck, *Polymer*, 46, (2005) 6369.

[26] M.S. Abbas-Abadi, M.N. Haghighi, H. Yeganeh and B. Bozorgi, *Journal of thermal analysis and calorimetry*, 114, (2013) 1333.

[27] Y. Zheng, L. Tao, X. Yang, Y. Huang, C. Liu and Z. Zheng, *Journal of Analytical and Applied Pyrolysis*, 133, (2018) 185.

[28] K. Murata, Y. Sakata and M. Brebu, *Journal of Analytical and Applied Pyrolysis*, 161, (2022) 105395.

[29] J.M. Saad, P.T. Williams, Y.S. Zhang, D. Yao, H. Yang and H. Zhou, *Journal of Analytical and Applied Pyrolysis*, 156, (2021) 105135.

[30] S. Kumar, A.K. Panda and R.K. Singh, *Resources, Conservation and Recycling*, 55, (2011) 893.

[31] S. Papari, H. Bamdad and F. Berruti, *Materials*, 14, (2021) 2586.

[32] B. Crist Jr, J. Oddershede, J. Sabin, J. Perram and M.A. Ratner, *Journal of Polymer Science: Polymer Physics Edition*, 22, (1984) 881.

[33] F.J. Vela, R. Palos, D. Trueba, J. Bilbao, J.M. Arandes and A. Gutiérrez, *Fuel Processing Technology*, 220, (2021) 106891.

[34] I. Vollmer, M.J. Jenks, M.C. Roelands, R.J. White, T. van Harmelen, P. de Wild, G.P. van Der Laan, F. Meirer, J.T. Keurentjes and B.M. Weckhuysen, *Angewandte Chemie International Edition*, 59, (2020) 15402.

[35] E. Rodríguez, G. Elordi, J. Valecillos, S. Izaddoust, J. Bilbao, J.M. Arandes and P. Castano, *Fuel Processing Technology*, 192, (2019) 130.

[36] M. Artetxe, G. Lopez, G. Elordi, M. Amutio, J. Bilbao and M. Olazar, *Industrial & Engineering Chemistry Research*, 51, (2012) 13915.

[37] M. Artetxe, G. Lopez, M. Amutio, G. Elordi, J. Bilbao and M. Olazar, *Chemical Engineering Journal*, 207, (2012) 27.

[38] A. Green and S. Sadrameli, *Journal of analytical and applied pyrolysis*, 72, (2004) 329.

[39] K. Murata, K. Sato and Y. Sakata, *Journal of Analytical and Applied Pyrolysis*, 71, (2004) 569.

[40] L. , J. Gu, Y. Wang, J. Zhang, H. Yuan and Y. Chen, *Chemical Engineering Journal*, 385, (2020) 123866.

[41] A. Kumari and S. Kumar, *Journal of Analytical and Applied Pyrolysis*, 124, (2017) 298.

[42] F. Mastral, E. Esperanza, P. Garcıa and M. Juste, *Journal of Analytical and Applied Pyrolysis*, 63, (2002) 1.

[43] M.d.R. Hernández, Á.N. García, A. Gómez, J. Agulló and A. Marcilla, *Industrial & engineering chemistry research*, 45, (2006) 8770.

[44] N.M. Ainali, D.N. Bikiaris and D.A. Lambropoulou, *Journal of Analytical and Applied Pyrolysis*, (2021) 105207.

[45] A. Mendes, A. Cunha and C. Bernardo, *Polymer Degradation and Stability*, 96, (2011) 1125.

[46] S. Al-Salem, M. Behbehani, A. Al-Hazza'a, J. Arnold, S. Alston, A. Al-Rowaih, F. Asiri, S. Al-Rowaih and H. Karam, *Journal of Material Cycles and Waste Management*, 21, (2019) 1106.

[47] A. Eschenbacher, F. Goodarzi, R.J. Varghese, K. Enemark-Rasmussen, S. Kegnæs, M.S. Abbas-Abadi and K.M. Van Geem, *ACS Sustainable Chemistry & Engineering*, (2021).

[48] M. Kusenberg, A. Eschenbacher, M.R. Djokic, A. Zayoud, K. Ragaert, S. De Meester and K.M. Van Geem, *Waste Management*, 138, (2022) 83.

[49] H.E. Toraman, T. Dijkmans, M.R. Djokic, K.M. Van Geem and G.B. Marin, *Journal of Chromatography A*, 1359, (2014) 237.

[50] N.D. Ristic, M.R. Djokic, A. Konist, K.M. Van Geem and G.B. Marin, *Fuel processing technology*, 167, (2017) 241.

[51] T. Dijkmans, K.M. Van Geem, M.R. Djokic and G.B. Marin, *Industrial & Engineering Chemistry Research*, 53, (2014) 15436.

[52] A. Zayoud, H. Dao Thi, M. Kusenberg, A. Eschenbacher, U. Kresovic, N. Alderweireldt, M. Djokic and K.M. Van Geem, *Waste Management*, 139, (2022) 85.

[53] M.T. Brouwer, E.U.T. van Velzen, A. Augustinus, H. Soethoudt, S. De Meester and K. Ragaert, *Waste management*, 71, (2018) 62.

[54] H. Dao Thi, M.R. Djokic and K.M. Van Geem, *Separations*, 8, (2021) 103.

[55] M. Roosen, N. Mys, M. Kusenberg, P. Billen, A. Dumoulin, J. Dewulf, K.M. Van Geem, K. Ragaert and S. De Meester, *Environmental Science & Technology*, 54, (2020) 13282.

[56] H. Bazgir, M.S. Abbas-Abadi, M.N. Haghighi, M.R.R. Darounkola, Z. Issaabadi and R. Rashedi, *Journal of Polymer Research*, 28, (2021) 1.

[57] A. Alem and M.D. Pugh, *International Journal of Applied Ceramic Technology*, 10, (2013) E258.

[58] N.S. Allen, L.J. Enriquez, M. Edge, C.M. Liauw, A. Parrondo and E. Fontan, *Journal of Vinyl and Additive Technology*, 7, (2001) 110.

[59] S. Moss and H. Zweifel, *Polymer degradation and stability*, 25, (1989) 217.

[60] R. Day, *Polymer Degradation and Stability*, 29, (1990) 73.

[61] E. Jakab and M. Blazsó, *Journal of analytical and applied pyrolysis*, 64, (2002) 263.

[62] M.O. Awan, A. Shakoor, M.S. Rehan and Y.Q. Gill, *Physica B: Condensed Matter*, 606, (2021) 412568.

[63] B. Smith, *Infrared spectral interpretation: a systematic approach*, CRC press, 2018, p.

[64] K.R. Jennings, 26, (1991) 813.

[65] V.J. Bruckman and K. Wriessnig, *Environmental Chemistry Letters*, 11, (2013) 65.

[66] S. Liang, H. Yang, K. Wang, Q. Zhang, R. Du and Q. Fu, *Acta Materialia*, 56, (2008) 50.

[67] D. Godshall, G. Wilkes, R.K. Krishnaswamy and A.M. Sukhadia, *Polymer*, 44, (2003) 5397.

[68] Y.M. Kim, C.H. Kim, J.K. Park, J.W. Kim and T.I. Min, *Journal of applied polymer science*, 61, (1996) 1717.

[69] P. Oblak, J. Gonzalez-Gutierrez, B. Zupančič, A. Aulova and I. Emri, *Polymer Degradation and stability*, 114, (2015) 133.

[70] A. D-90, *Annual Book of Standards*, (2015).

[71] J. Wang, J. Jiang, J. Ding, X. Wang, Y. Sun, R. Ruan, A.J. Ragauskas, Y.S. Ok and D.C. Tsang, *Journal of Cleaner Production*, 314, (2021) 127966.

[72] H. Hinsken, S. Moss, J.-R. Pauquet and H. Zweifel, *Polymer degradation and stability*, 34, (1991) 279.

[73] J.D. Winkler, *Chemical reviews*, 96, (1996) 167.

[74] İ. Çit, A. Sınağ, T. Yumak, S. Uçar, Z. Mısırlıoğlu and M. Canel, *Polymer Bulletin*, 64, (2010) 817.

[75] V. Kislov, A. Sadovnikov and A. Mebel, *The Journal of Physical Chemistry A*, 117, (2013) 4794.

[76] M. Guisnet and P. Magnoux, *Applied Catalysis A: General*, 212, (2001) 83.

[77] R.K. Singh, B. Ruj, A.K. Sadhukhan and P. Gupta, *Journal of Environmental Management*, 239, (2019) 395.

[78] T. Menares, J. Herrera, R. Romero, P. Osorio and L.E. Arteaga-Pérez, *Waste management*, 102, (2020) 21.

[79] S.S.Z. Salmasi, M.S. Abbas-Abadi, M.N. Haghighi and H. Abedini, *Fuel*, 160, (2015) 544.

[80] S.E. Barrows and T.H. Eberlein, *Journal of chemical education*, 82, (2005) 1329.

[81] L. Ballice and R. Reimert, *Chemical Engineering and Processing: Process Intensification*, 41, (2002) 289.

[82] P. Kusch, D. Schroeder-Obst, V. Obst, G. Knupp, W. Fink and J. Steinhaus, in *Handbook of Materials Failure Analysis With Case Studies From the Chemicals, Concrete and Power Industries*, Elsevier, 2016, p. 441.

[83] R. Pan, J.V.F. Duque and G. Debenest, *Waste and Biomass Valorization*, 12, (2021) 2623.

[84] M. Sablier, M. Šala, Y. Kitahara, S. Takahasi and T. Fujii, *Journal of Analytical and Applied Pyrolysis*, 89, (2010) 178.

[85] M.S. Abbas-Abadi, K.M. Van Geem, J. Alvarez and G. Lopez, *Journal of Thermal Analysis and Calorimetry*, (2021) 1.

[86] D. Nohara and T. Sakai, *Industrial & engineering chemistry research*, 31, (1992) 14.

[87] S. Müller, Y. Liu, M. Vishnuvarthan, X. Sun, A.C. van Veen, G.L. Haller, M. Sanchez-Sanchez and J.A. Lercher, *Journal of Catalysis*, 325, (2015) 48.

[88] J. Towfighi, M. Sadrameli and A. Niaei, *Journal of chemical engineering of Japan*, 35, (2002) 923.

[89] P.A. Willems and G.F. Froment, *Industrial & engineering chemistry research*, 27, (1988) 1959.

[90] M.E. O'Reilly, S. Dutta and A.S. Veige, *Chemical reviews*, 116, (2016) 8105.

[91] Ž. Olujić, in *Distillation*, Elsevier, 2014, p. 295.

[92] J. Ruan, J. Huang, B. Qin and L. Dong, *ACS Sustainable Chemistry & Engineering*, 6, (2018) 5424.

[93] R. Miranda, H. Pakdel, C. Roy and C. Vasile, *Polymer Degradation and Stability*, 73, (2001) 47.

Declaration of interests ☐The authors declare that they have no known competing financial interests or personal relationships that could have appeared to influence the work reported in this paper. ☒The authors declare the following financial interests/personal relationships which may be considered as potential competing interests:

Kevin M. Van Geem reports was provided by Ghent University.

Highlights:

- Pyrolysis of virgin and waste high density polyethylene.
- Comprehensive two-dimensional gas chromatography coupled to various detectors.
- Providing a comprehensive kinetic model using a unique quantum study.
- Double bond and tertiary carbon as effective structural parameters.
- Investigating the influential mechanisms in polyethylene pyrolysis.